Journal of Alloys and Compounds 511 (2012) 81–84

Contents lists available at ScienceDirect

Journal of Alloys and Compounds

journal homepage: www.elsevier.com/locate/jallcom

Effects of pelletization of reactants and diluents on the combustion synthesis of Si_3N_4 powder

Jianhui Yang[a,b], Linsen Han[a,b], Yixiang Chen[a], Guanghua Liu[a], Zhiming Lin[a], Jiangtao Li[a,*]

[a] *Technical Institute of Physics and Chemistry, Chinese Academy of Sciences, Beijing 100190, China*
[b] *Graduate School of the Chinese Academy of Sciences, Beijing 100049, PR China*

ARTICLE INFO

Article history:
Received 25 May 2011
Received in revised form 7 August 2011
Accepted 8 August 2011
Available online 19 August 2011

Keywords:
Si_3N_4
Combustion synthesis
SHS
Pelletized reactants

ABSTRACT

Reactants were pelletized, and then combustion synthesis of Si_3N_4 powder was achieved under the N_2 pressure of 3.0 MPa. Effects of the pelletization of reactants and Si_3N_4 diluents on the combustion process parameters and the characteristics of products were studied. The combustion mode of single reactant pellet was preliminarily discussed. The results indicated that the combustion reaction of single pellet was layer-by-layer from the surface to the core, which led to two peaks on the combustion temperature variation waves. With increasing the diluents content, the morphologies of Si_3N_4 particles changed from short rods into equiaxed grains, and residual Si in the final products obviously decreased. Single phase β-Si_3N_4 powder mainly contained equiaxed grains was prepared when 58 wt.% diluents was added.

1. Introduction

Silicon nitride (Si_3N_4) ceramics have been acknowledged as one of the most promising structural materials because of their excellent mechanical properties at both room and high temperature, good resistance to oxidation and thermal shock, outstanding creep resistance and wear resistance [1–5]. Nevertheless, a wider use of Si_3N_4 ceramics is still restricted owing to the cost of their synthesis and final processing. Direct nitridation, carbothermic reduction, vapor-phase reactions and thermal decomposition are the most commonly used processes for fabricating Si_3N_4 powder, which usually require high energy contributions and long periods of nitridation time [4–8]. Synthesis of Si_3N_4 powder by combustion synthesis (CS), commonly known as the self-propagating high-temperature synthesis (SHS), has attracted attention for the last few years, as this technique provides lower processing cost, easier preparation and higher product purity compared with conventional methods [9–13].

As described previously [14,15], reactants of combustion synthesis were loaded indirectly and loosely into the graphite after milling. Because of this, the porosity of green body that was quite important to the infiltration combustion of gas–solid system was very difficult to control. However, the pelletization of Si powder or Si/Si_3N_4 is not only benefit for simply loading reactants but also easy to regulate the porosity of green body. Jovanovic studied the kinetics of direct nitridation of Si using pelletized Si grains in a fluidized bed. Silicon pellets that replaced powder particles as reactants promoted the final conversion of Si because of large amount of porosity formed during the fluidized-bed nitridation process [16]. Up to now, the synthesis of Si_3N_4 powder with pelletized reactants grains using the SHS technique has not been reported. Meanwhile, although the roles of Si_3N_4 diluents in the combustion synthesis of Si_3N_4 powder have been widely studied [10–13], effects of diluents on the combustion process of reactant pellets and the characteristics of final products have not been investigated before.

In the present work, pellets of Si/Si_3N_4 with constant size were prepared, Si_3N_4 powder was fabricated by combustion synthesis using these pellets. The characteristics of combustion process of pelletized reactants and effects of Si_3N_4 diluents on the features of the final products were studied. The combustion mode of single reactant pellet was also preliminarily discussed.

2. Experimental procedure

Si powder (325 mesh, >99.9 wt.%, Fushun Al Factory, China), Si_3N_4 powder (β-ratio >90 wt.%, self-fabricated by SHS) were used as the raw materials. Polyvinyl alcohol (PVA, $n = 1750 \pm 50$, Sinpharm Chemical Reagent Co., Ltd., China) was used as the binder for preparing reactant pellets.

These raw materials weighed according to the compositions in the Table 1 were attrition milled for 1 h using steel balls as the milling media with a ball/charge weight ratio of 8:1. The mixed powders were sieved through a 200 mesh screen and then put into the revolving container of the chufa style sugar coater. Appropriate content of 0.5 wt.% PVA solution was slowly sprinkled into the container in a pray using a water sprinkler. The raw pellets were taken out from the revolving container after 30 min and sieved through different sizes of mesh screens. Reactant pellets with the sizes of 0.7–1.0 mm were obtained. Then, these pellets were dried and loosely packed in a porous graphite crucible. The crucible was then placed into a stainless

---

[*] Corresponding author. Tel.: +86 10 82543695; fax: +86 10 82543695.
E-mail address: ljt0012@vip.sina.com (J. Li).

0925-8388/$ – see front matter © 2011 Elsevier B.V. All rights reserved.
doi:10.1016/j.jallcom.2011.08.057

Table 1
Starting materials compositions and N_2 pressures of combustion synthesis.

Sample	Composition (wt.%) $Si:Si_3N_4$	P_{N_2} (MPa)
A1	100:0	3.0
A2	95:5	3.0
A3	67:33	3.0
A4	60:40	3.0
A5	50:50	3.0
A6	42:58	3.0

steel combustion reaction chamber. After evacuation, the reaction chamber was inflated with high-purity N_2 to 3.0 MPa. The combustion reaction was triggered by passing an electric current through a tungsten coil closely above the sample. The reaction temperatures were measured by W-R3/W-Re25 thermocouples which were inserted into the center of the sample and connected with a computer system of data treatment.

The phase composition was determined by X-ray diffraction (XRD; Cu Kα, Rigaku, Japan) and the microstructure was observed by scanning electron microscopy (SEM; JSM-6460LV, JEOL, Japan).

3. Results and discussion

3.1. Reaction characteristics of combustion synthesis using reactant pellets

Fig. 1 shows the temperature variation curves of sample A5 during the combustion synthesis process. It could be seen that the temperature sharply increased to the highest value, and after transitorily decreasing, another highest temperature peak about 2215 °C was observed. Then, it began to decrease. Both of temperature variations in measured location were very similar, and every temperature curve was bimodal (see the inset image in Fig. 1). According to calculation, time interval (Δt) of heat transfer from the first thermocouple to another was 1.24 min, and the combustion wave propagation velocity (V_c) was about 5.6 cm/min. Temperature variation curves of other samples which had not been listed here were extraordinarily similar with Fig. 1.

Fig. 2 is the schematic diagram of combustion synthesis using reactant pellets. After the green body was ignited, the combustion front that could be considered as the reaction area would propagate from a head of compact towards another head. Behind the reactive area, the combustion product was fabricated that mainly contained lots of product pellets. The reaction heat (Q_r) usually transferred from reactive area to the reactant area, which was used to preheat and ignite the starting materials. After preheated and ignited, the small Si grains adhered on the surface of pellets would be reacted with N_2 first. Because of the rich resources of N_2, reactants on the surface layer of a pellet would be reacted quickly, and a lot of reaction heat was released sharply which led to the first peak of every combustion temperature curve. As Varma described [17], heat conduction through the solid phase was often considered to be the dominant mechanism during combustion in heterogeneous media, since conductivity of solid phase was several orders of magnitude higher than that of gas phase in voids. The reaction heat (Q_r) produced by surface combustion of the pellet would transfer towards the interior Si grains with the closest contact, which resulted in the combustion micro-front propagating to the core of the pellet (see the image of I in Fig. 2). During this process, the temperature that thermocouple measured would decrease slightly, which was found in Fig. 1. When Si grains in the center of the pellet had be ignited, large amount of reaction heat (Q_r) from the whole pellet would transfer around (see the image of II in Fig. 2), which corresponded to the second peak of temperature curves in Fig. 1. Due to the modes of heat transfer and combustion micro-front propagation, combustion of the whole compact proceeds by two sequential steps: rapid reaction of a single pellet, followed by an ignition delay during which preheating of the neighboring pellet occurs. This model, named as relay-race mechanism by Varma, had the features that the reaction front movement consisted of a series of rapid jumps and hesitations and the instantaneous velocity distribution was not unimodal [17]. Therefore, the information obtained from the combustion zone by thermocouples had two highest values (see Fig. 1), which accorded with the mechanism well.

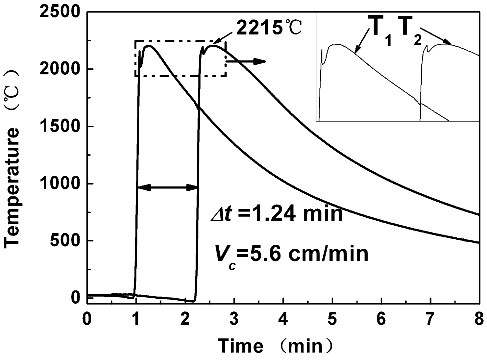

Fig. 1. Temperature variation curves of sample A5 during the combustion synthesis process T_1, temperature curve measured by thermocouple 1; T_2, temperature curve measured by thermocouple 2; Δt, time interval of thermal transfer between thermocouples; V_c, combustion wave speed.

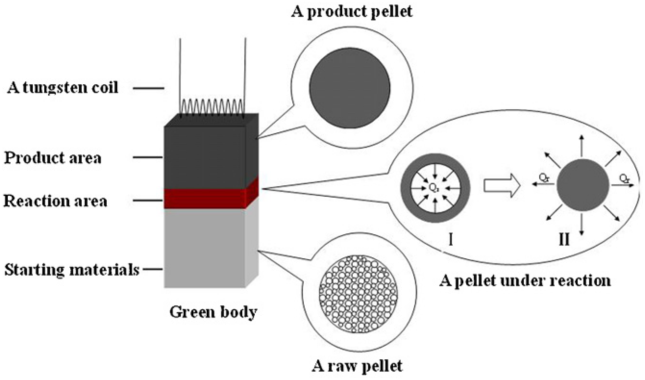

Fig. 2. The schematic diagram of combustion synthesis Q_r, reaction heat.

3.2. Phase compositions of combustion synthesis products

The XRD patterns of the combustion products are showed in Fig. 3. It was found that α-Si_3N_4, β-Si_3N_4 and residual Si were present in the products of A1 and A2, and the sample A3 contained α- and β-Si_3N_4. However, XRD patterns of samples A4, A5 and A6 only included diffraction peaks of β-Si_3N_4. A change in amount of residual Si, not detected by XRD in A3–A6, could be

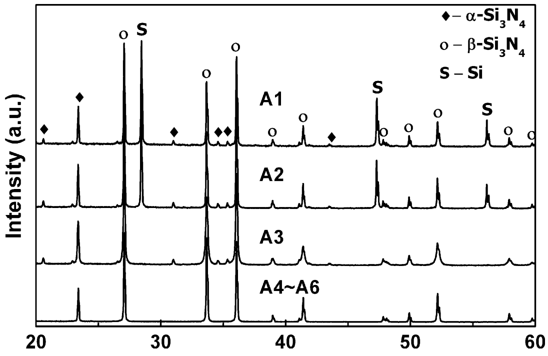

Fig. 3. X-ray diffraction (XRD) patterns of the combustion products.

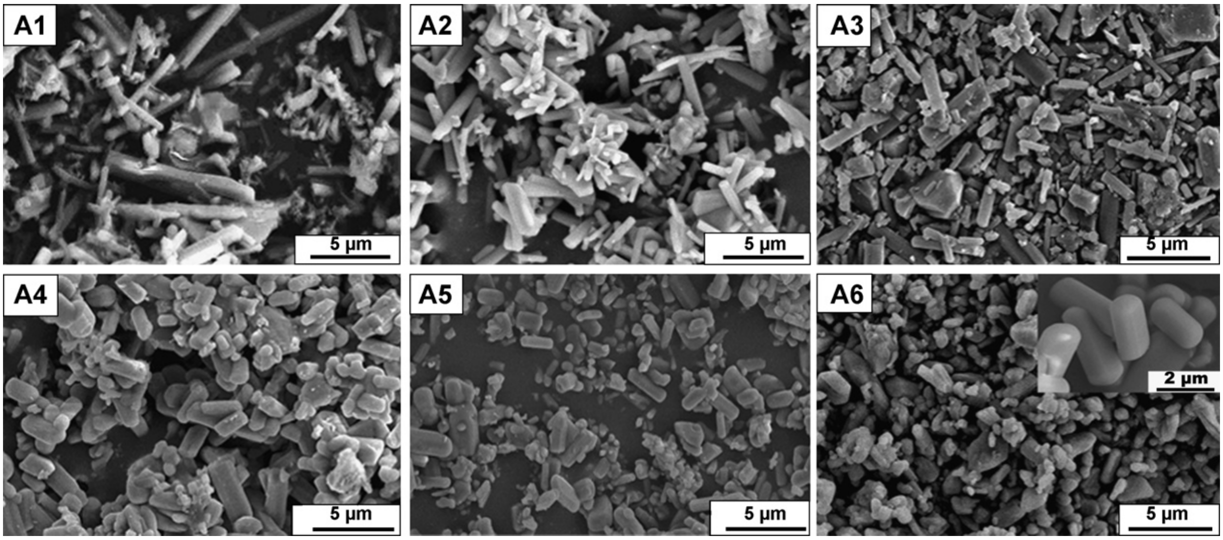

Fig. 4. Scanning electron microscope (SEM) photographs of combustion synthesized products.

Table 2
Combustion process parameters and phase compositions of the final products.

Sample	Process parameter		Phase composition
	T_{max} (°C)	V_c (cm/min)	
A1	2285 6.1	6.1	α-Si_3N_4, β-Si_3N_4, residual Si
A2	2250 5.9	5.9	α-Si_3N_4, β-Si_3N_4, residual Si
A3	2247 5.9	5.9	α-Si_3N_4, β-Si_3N_4
A4	2236 5.8	5.8	β-Si_3N_4
A5	2215 5.6	5.6	β-Si_3N_4
A6	2197 5.1	5.1	β-Si_3N_4

associated with contents of diluents, Si_3N_4, added in starting materials. It is suggested that complete nitridation of Si was achieved when the content of diluents was larger than 33 wt.%. The effects of diluents on combustion synthesis of Si_3N_4 powder were reported elsewhere [10–13]. Meanwhile, with increasing of diluents content, α phase is decreasing. This could not be only attributed to the decrease of combustion temperature. Temperature values of all the samples A1–A6 were above 2000 °C, which were listed in Table 2. Under these temperatures, α-Si_3N_4 fabricated newly converted to β-Si_3N_4. Although the temperatures of A1–A3 were higher and more Si melts were present, more α-Si_3N_4 was formed from the vapour transport material [18], since more Si vapour was present than samples A4–A6.

3.3. Particles morphology of combustion synthesis products

The SEM photographs of combustion products are shown in Fig. 4. We could see that most of Si_3N_4 particles of samples A1–A6 were rod-like shape, and the ratios of long and radius of Si_3N_4 particles were decreasing with increasing the addition content of Si_3N_4 diluents in starting materials. Si_3N_4 rods in samples A1 and A2 were longer than those in other samples, and lots of them were agglomerated together. This could be related with the present of Si melts and coalescence during the high temperature combustion reaction. The agglomeration of Si melts inhibited the infiltration of nitrogen from outside the reactant compact, which leaded to that residual Si was found in final products. The length and aspect ratio of rod-like crystals increased with increasing amount of Si melts.

Short columnar crystals and small ball-like particles with better dispersion were found in samples A4, A5 and A6. Especially, most of particles in sample A6 were small equiaxed grains with the round tips (see the inset image in Fig. 4A6). The change in the morphologies of A1–A6 could be associated with addition content of Si_3N_4 diluents in the starting materials. As the combustion temperature decreased with increasingly adding Si_3N_4 diluents, the content of Si melts obviously reduced, which leaded to not only the better particle distribution but also the complete conversion of Si grains and effectively limited the growth of Si_3N_4 crystals along the direction of *c* axis. As the content of diluents was 58 wt.%, the uniform sizes of Si_3N_4 particles with smooth surfaces were smaller than 2 μm.

4. Conclusion

Combustion synthesis of Si_3N_4 powder was carried out using pelletized reactants under the N_2 pressure of 3.0 MPa. The pelletization of reactants and the addition contents of Si_3N_4 diluents obviously affected the combustion process parameters and the characteristics of products. The combustion reaction of single pellet was layer-by-layer from the surface to the center, which led to the rapid nitridation with the combustion wave velocity of about 5.6 cm/min and the combustion temperature of 2215 °C in sample A5. Meanwhile, the combustion temperature variation waves were bimodal, which had the good agreement with the relay-race mechanism of reaction wave propagation. Complete conversion of Si powder was achieved when more than 33 wt.% Si_3N_4 diluents was added in the reactants. The length of Si_3N_4 rod-like particles continuously decreased with increasing the diluents content because of less Si melts in the system. β-Si_3N_4 powder with the uniform particle sizes smaller than 2 μm was prepared when 58 wt.% diluents was added.

Acknowledgements

The financial supports from the following projects are greatly appreciated: Key Laboratory of Functional Crystals and Laser Technology, TIPC, CAS; National Natural Science Foundation Key Project, Nos. 50502035 and 50372074.

References

[1] N. Shibata, S.J. Pennycook, T.R. Gosnell, G.S. Painter, W.A. Shelton, P.F. Becher, Nature 428 (2004) 730–733.
[2] F.L. Riley, J. Am. Ceram. Soc. 83 (2) (2000) 245–265.
[3] H. Lange, G. Wotting, G. Winter, Angew. Chem. Int. Ed. Engl. 30 (1991) 1579–1597.
[4] H.I. Won, C.W. Won, H.H. Nersisyan, K.S. Yoon, J. Alloys Compd. 496 (2010) 656–659.

[5] D.Y. Chen, B.L. Zhang, H.R. Zhuang, W.L. Li, S.Y. Xu, Mater. Lett. 57 (2002) 399–402.
[6] A. Atkinson, A.J. Moulson, E.W. Roberts, J. Am. Ceram. Soc. 59 (7–8) (1976) 285–289.
[7] T. Licko, V. Figusch, J. Puchyova, J. Eur. Ceram. Soc. 9 (1992) 219–230.
[8] T. Yamada, Am. Ceram. Soc. Bull. 72 (1993) 99–106.
[9] C.L. Yeh, F.S. Wu, Y.L. Chen, J. Alloys Compd. 509 (2011) 3985–3990.
[10] I.G. Cano, S.P. Baelo, M.A. Rodriguez, S.D. Aza, J. Am. Ceram. Soc. 21 (2001) 291–295.
[11] K. Hirao, Y. Miyamoto, M. Koizumi, J. Am. Ceram. Soc. 69 (4) (1986) C-C60–C-C61.
[12] Z.A. Munir, J.B. Holt, J. Mater. Sci. 22 (1987) 710–714.
[13] I.G. Cano, I.P. Borovinskaya, M.A. Rodriguez, V. Grachev, J. Am. Ceram. Soc. 85 (9) (2002) 2011–2209.
[14] Y.G. Cao, C.C. Ge, Z.J. Zhou, J.T. Li, J. Mater. Res. 14 (3) (1999) 876–880.
[15] Y.X. Chen, Z.M. Lin, J.T. Li, J.S. Du, S.L. Yang, J. Eur. Ceram. Soc. 28 (2008) 289–293.
[16] Z.R. Jovanovic, J. Mater. Sci. 33 (1998) 2339–2355.
[17] A. Varma, A.S. Mukasyan, S. Hwang, Chem. Eng. Sci. 56 (2001) 1459–1466.
[18] H.M. Jennings, M.H. Richman, J. Mater. Sci. 11 (1976) 2087–2098.